TCABSE-J Research Article

ISSN: 2583- 2557, *Volume 2, Issue 1, pp16-22. 2026.*

TCABSE-J Interdisciplinary Sciences Journal

In vitro screening for the optimal biochemical conditions of lysozyme liquid-liquid phase separation vs. crystallization using vapor drop diffusion method.

Pravallika Lankapalli[1, 2], Sahithi Netala[1, 2], Manikanta Sodasani[1], Jahnavi Chintalapati[1, 2] and Ravikiran S. Yedidi[1, *]

[1]Department of Intramural research core, The Center for Advanced-Applied Biological Sciences & Entrepreneurship (TCABS-E), Visakhapatnam 530003, A.P. India; [2]Department of Biochemistry, Andhra University, Visakhapatnam 530003, A. P. India. (*Correspondence to R.S.Y.: tcabse.india@gmail.com).

Keywords: Lysozyme, protein crystallization, LLPS, hanging drop vapor diffusion, grid screens, 24-well plates.

Protein liquid-liquid phase separation (LLPS) has gained plenty of research interests in the past decade. LLPS was observed as a natural phenomenon that occurs in cells to facilitate the biochemical processes to continue without interruptions, especially in conditions such as stress, senescence, etc. In this study, we hypothesized that by using a model protein such as the hen egg white Lysozyme (HEWL) one can screen various sets of biochemical conditions and identify the optimal ones for obtaining the LLPS of the HEWL in order to mimic the intracellular biochemical processes and successfully carry them out in vitro. However, HEWL is known to crystallize well in several biochemical conditions so the current study focuses on the optimal conditions where the HEWL can produce LLPS but not crystals. Sodium chloride and ammonium sulfate grid screens were used in combination with the vapor diffusion hanging drop methodology. Several hits were identified and discussed.

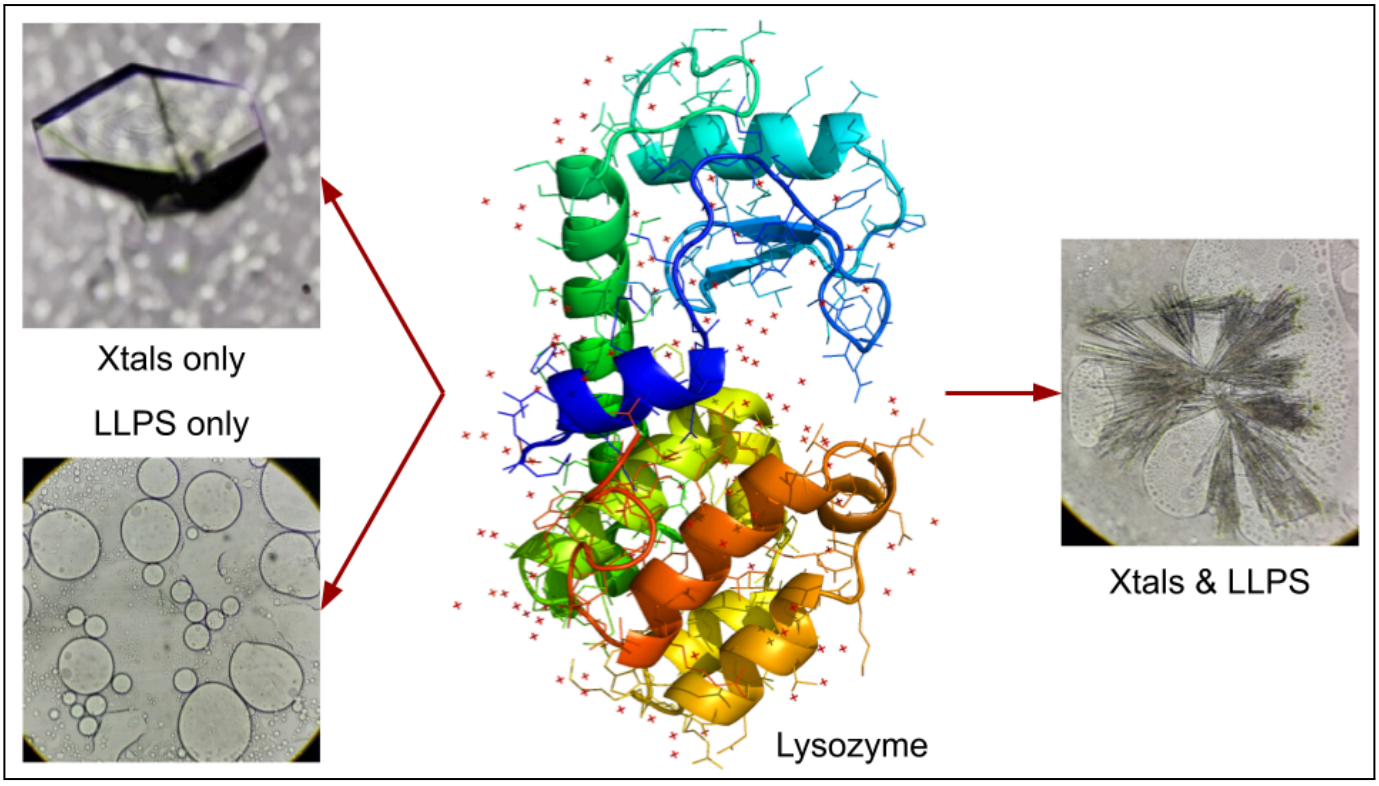

Figure 1. Hen egg white lysozyme yields either crystals or LLPS separately under different conditions or combinedly in a single condition.

Citation: Lankapalli, P., Netala, S., Sodasani, M., Chintalapati, J. and Yedidi, R.S. (2026). *In vitro* screening for the optimal biochemical conditions of lysozyme liquid-liquid phase separation vs. crystallization using vapor drop diffusion method. *TCABSE-J*, Vol. 2, Issue 2:16-22. Epub: April 6th, 2026.

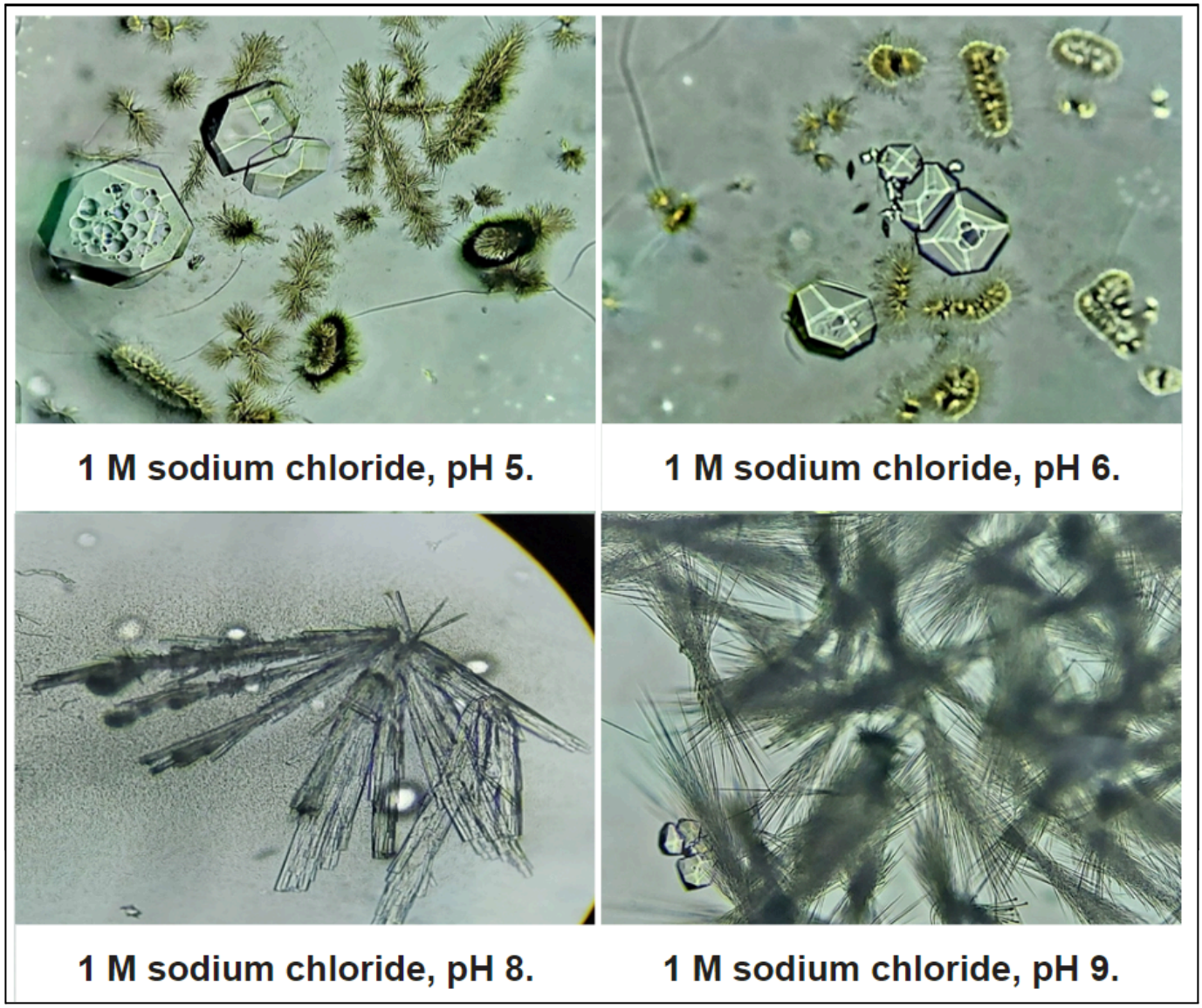

Figure 2. Crystals of lysozyme in different morphologies obtained in the sodium chloride grid screen (at various pH values) using the hanging drop vapor diffusion method in a 24-well plate at room temperature within 2 months.

LLPS Liquid-liquid phase separation (LLPS) is a thermodynamically driven, reversible phenomenon consisting of demixing into two distinct liquid phases with different solute concentrations. Emerging evidence suggests that LLPS is a vital and pervasive phenomenon underlying the development of membrane-less organelles in eukaryotic cells. LLPS is gaining acceptance as a powerful mechanism to explain the formation of membrane-less organelles and their functions. Our everyday experience with water and oil droplets illustrates a simple LLPS. In Biology, cells resemble liquid droplets that maintain membrane-less compartments, important for concentrating certain molecules and facilitating spatiotemporal regulation of cellular functions. Recent studies have revealed evidence that indicates that LLPS plays a vital role in human health and disease. This highlights the need for an overview of the recent advances in the field to translate our current knowledge regarding LLPS into therapeutic discoveries. Recent studies have shown that membrane-less organelles and compartments in the cell are assembled via LLPS. *In vitro* LLPS assays using recombinant expressed and purified proteins are necessary for us to further understand how the assembly of phase-separated compartments is regulated in the cells.

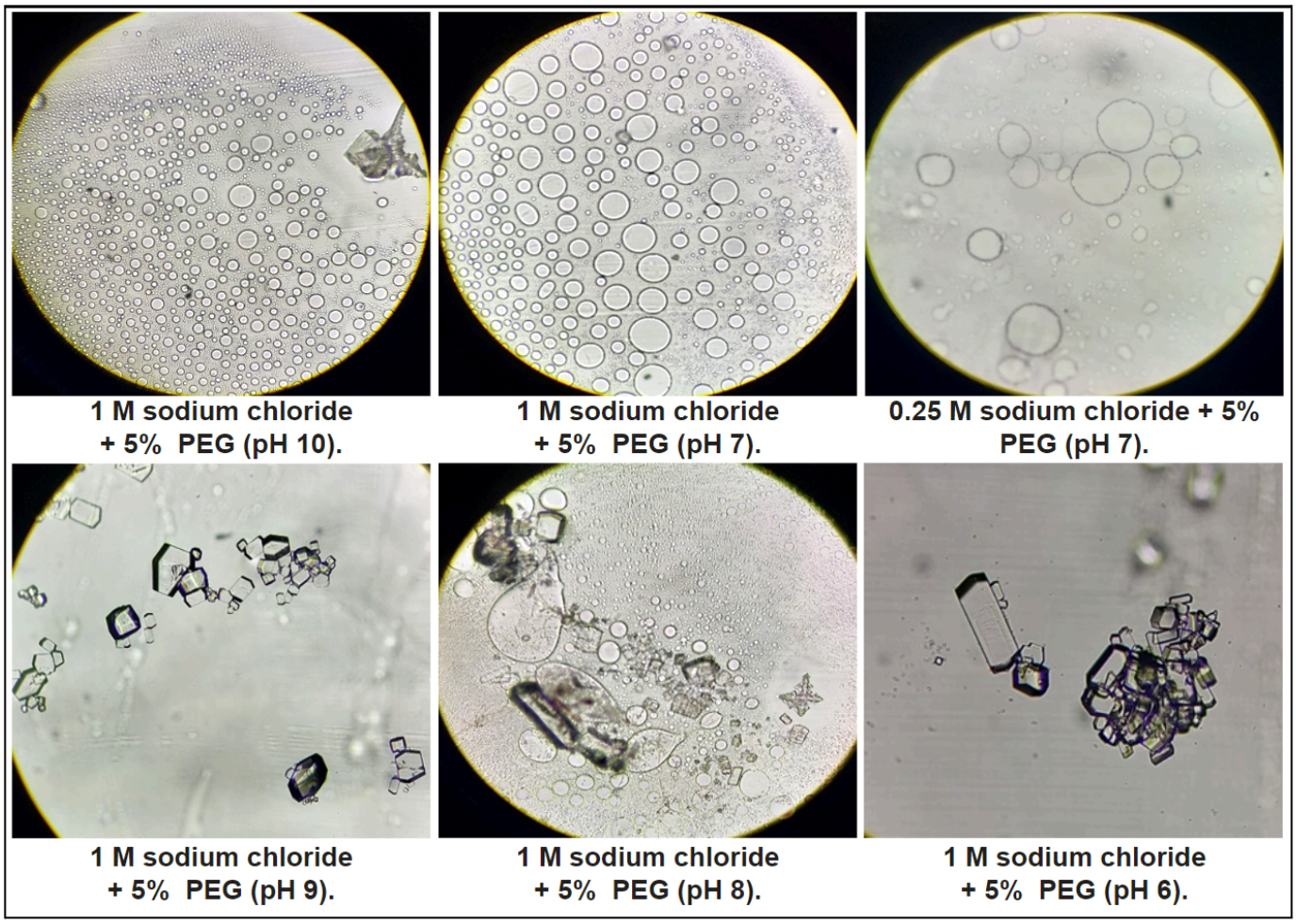

Figure 3. Lysozyme behavior in NaCl grid+5% PEG w.r.t. pH.

Protein LLPS is a growing research field in cell biology and many other techniques are being used to study this phenomenon such as NMR, cryo-EM and single molecule fluorescence methods. Improvements in technology will drive developments in the field of protein LLPS [1]. LLPS has drawn increasing attention in understanding biological processes. Ming *et al*. demonstrated that cancer may be more sensitive and more addictive to LLPS, which suggests the therapeutic potential of LLPS in cancer [2]. Condensates formed via LLPS provide specific local environments for broad cellular activities [3, 4]. With the elucidation of the function of LLPS within cells, utilizing this phenomenon to intervene cell activities has great potential for biomedical applications. Until recently the discovered phase separation phenomena in living organisms were restricted intracellularly, as a crowded environment inside of cells is critical for LLPS. This limits the prospect of LLPS in drug development [5]. The LLPS of intrinsically disordered proteins is a commonly observed phenomenon within the cell. Such condensates are also highly attractive for applications in biomaterials.

In this study, we utilized the hen egg white lysozyme (HEWL) as a model protein to systematically evaluate the optimal biochemical conditions to identify the hits where the HEWL yields clear drop (or) precipitate (or) LLPS (or) crystals. Pure HEWL was purchased from HiMedia Laboratories and was used at a very high concentration on purpose to see whether crystallization would dominate over the formation of LLPS. This evaluation was performed using the standard hanging drop vapor diffusion method in the 24-well plates. The typical ammonium sulfate, sodium chloride and sodium malonate grid screens containing a range of buffer strengths (1 M, 0.5 M, 0.25 M and 0.125 M) at different pH values (pH-5, pH-6, pH-7, pH-8, pH-9 and pH-10) were used for screening either with or without a 5% polyethylene glycol (PEG) mixing. All plates were tested at room temperature with a protein to buffer ratio of 1:1. Periodic microscopic observations were performed.

Figure 4. LLPS of HEWL in ammonium sulfate (0.125 M).

Materials & Methods:

Lysozyme preparation: The protein used for the analysis is commercially available hen egg white lysozyme (HEWL) without any further purification. Stock solution for lysozyme is prepared by dissolving 2 mg of pure lysozyme powder in 1 ml of deionised water to achieve a concentration of 2 mg/ml.

Buffer preparation: Solutions of Ammonium sulfate, sodium chloride, sodium malonate, PEG, 1N HCl and 1N NaOH were prepared for screening. Ammonium sulfate buffers were prepared at 4 different molarities (1 M, 0.5 M, 0.25 M and 0.125M) and at 6 different pH values viz. 5-10. The 1M ammonium sulfate buffers were prepared by dissolving 6.6 g of ammonium sulfate in each 50 ml of deionised water and different pH -5,6,7,8,9,10 are adjusted by 1N HCl and 1N NaOH. The 0.5 M ammonium sulfate buffers were prepared by dissolving 3.3 g of ammonium sulfate in each 50 ml of deionised water and different pH-5,6,7,8,9,10 are adjusted by 1N HCl and 1N NaOH. The 0.25 M ammonium sulfate buffers were prepared by dissolving 1.7 g of ammonium sulfate in each 50 ml of deionised water and different pH-5,6,7,8,9,10 are adjusted by 1N HCl and 1N NaOH. The 0.125 M ammonium sulfate buffers were prepared by dissolving 0.83 g of ammonium sulfate in each 50 ml of deionised water and different pH-5,6,7,8,9,10 are adjusted by 1N HCl and 1N NaOH.

Sodium chloride buffers are prepared at 4 different molarities (1 M, 0.5 M, 0.25 M and 0.125M) and at 6 different pH values (5-10). The 1 M sodium chloride buffers were prepared by dissolving 2.9 g of sodium chloride in each 50 ml of deionised water and different pH-5,6,7,8,9,10 are adjusted by 1N HCl and 1N NaOH. The 0.5 M sodium chloride buffers were prepared by dissolving 1.5 g of sodium chloride in each 50 ml of deionised water and different pH-5,6,7,8,9,10 are adjusted by 1N HCl and 1N NaOH. The 0.25 M sodium chloride buffers were prepared by dissolving 0.7 g of sodium chloride in each 50 ml of deionised water and different pH-5,6,7,8,9,10 are adjusted by 1N HCl and 1N NaOH. The 0.125M sodium chloride buffers were prepared by dissolving 0.4 g of sodium chloride in each 50 ml of deionised water and different pH-5,6,7,8,9,10 are adjusted by 1N HCl and 1N NaOH.

Sodium malonate buffers are prepared at 4 different molarities (3.4 M, 1.7 M, 0.85 M and 0.425 M) and at 6 different pH values (5,6,6.5,7,7.5,8). The 3.4 M sodium malonate buffers were prepared by dissolving 5 g of sodium malonate in each 10 ml of deionised water and different pH-5,6,6.5,7,7.5,8 are adjusted by 1N HCl and 1N NaOH. The 1.7 M sodium malonate buffers were prepared by dissolving 2.5 g of sodium malonate in each 10 ml of deionised water and different pH-5,6,6.5,7,7.5,8 are adjusted by 1N HCl and 1N NaOH. The 0.85 M sodium malonate buffers were prepared by dissolving 1.25 g of sodium malonate in each 10 ml of deionised water and different pH-5,6,6.5,7,7.5,8 are adjusted by 1N HCl and 1N NaOH. The 0.425 M sodium malonate buffers were prepared by dissolving 0.63 g of sodium malonate in each 10 ml of deionised water and different pH -5,6,6.5,7,7.5,8 are adjusted by 1N HCl and 1N NaOH. PEG (0.05 g) was added to prepare all the buffers with 5% PEG.

Setting up hanging drops for vapor diffusion: In order to screen various conditions using the buffers prepared above, the hanging drop vapor diffusion method was used in 24-well plates. Five 24-well plates are labeled with ammonium sulfate, sodium chloride, sodium malonate, ammonium sulfate with PEG, sodium chloride with PEG with their respective concentrations and pH values. Except for sodium malonate, remaining buffers each 1 ml are filled into the wells. Cover slips were prepared by mixing equal volume 2 µL of lysozyme solution with 2 µL of the well solution (1:1 ratio) the slip would be placed over. The coverslips were inverted over the wells, which were sealed with vaseline, so as to create a closed system. Water from the droplet diffuses to the reservoir at the bottom of the well, causing an increase in precipitant concentration optimal for protein crystallization and LLPS within the drop. The five 24-well plates are incubated at room temperature without any movement for a few days.

Imaging with microscope: In order to check the final results, each coverslip was removed from the well and visualized under the microscope (10X magnification) and observed for the formation of crystals/LLPS. The obtained results were analyzed carefully. Images were taken for hits for both crystals and LLPS conditions from all plates. The images were labeled with the details of each condition at which the image was taken.

Results:

LLPS vs. Crystallization hits in sodium chloride: The 24-well plates with buffers were observed under the light microscope.

TCABSE-J Research Article
ISSN: 2583- 2557, *Volume 2, Issue 1, pp16-22. 2026.*

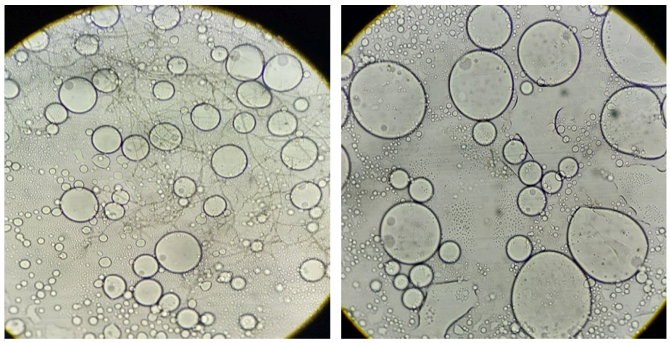

Figure 5. LLPS ammonium sulfate + 5% PEG.

The sodium chloride buffer containing 24-well plates were observed. Most of them were crystals with variable morphologies rather than LLPS observations. The lysozyme crystals obtained at pH values 5, 6, 7 and 8 with 1 M sodium chloride buffer are shown in Fig. 2. However, addition 5% of PEG to sodium chloride yielded LLPS formations in a few conditions as shown Fig. 3.

LLPS vs. Crystallization hits in ammonium sulfate: The LLPS condensates observed at 0.125 M concentration and pH 6 of ammonium sulfate as a buffer (Fig. 4). Similar LLPS condensates were observed at 0.125 M concentration of ammonium sulfate as a buffer and pH values of 7, 8, 9 and 10. Next ammonium sulfate with 5% PEG buffer-containing 24-well plates were observed. LLPS were obtained at pH values, 5 and 6 with 1 M ammonium sulfate + 5% PEG as shown in Fig. 5.

LLPS vs. Crystallization hits in sodium malonate: The sodium malonate containing 24-well plates were observed for the formation of LLPS/crystals. The lysozyme crystals were obtained at pH 5 with 0.85 M and 0.425 M sodium malonate concentrations are shown in Fig. 6. No LLPS hits were seen with sodium malonate without PEG. Interestingly, the addition of 5% PEG resulted in both LLPS and crystals at pH10 within the same drop (Fig. 7).

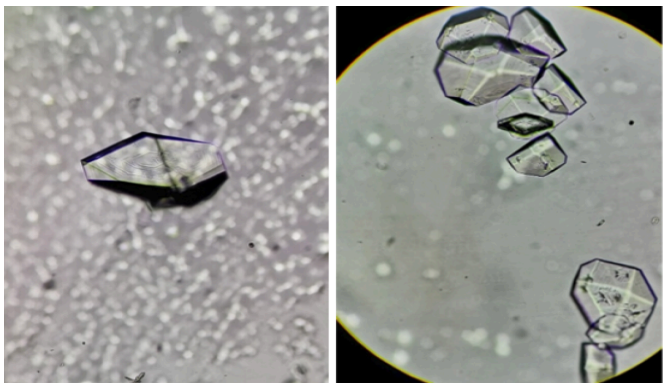

Figure 6. HEWL crystals in sodium malonate grid screen (0.85 M and 0.425 M) at pH 5.0.

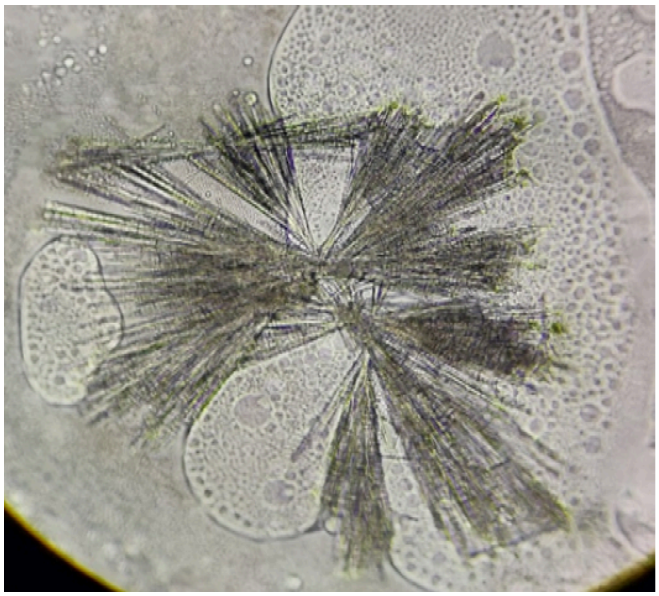

Figure 7. Crystals and LLPS of HEWL in 0.5 M sodium malonate + 5% PEG at pH 10.

Discussion:

Condensates are formed at the biochemical conditions at pH 6, 7, 8, 9, 10 at 0.125M concentration respectively. Lysozyme crystals are obtained at several biochemical conditions with different morphologies. Systematically, lysozyme crystal was observed at 1 M ammonium sulfate buffer at pH 5. Lysozyme crystals were further obtained at 1 M sodium chloride buffer at pH 5, 6, 8 and 9. The number for crystals decreased as the pH of the buffer increased. Lysozyme crystals were observed at 0.85 M and 0.425 M sodium malonate buffer at pH 5 but single crystals were observed at 0.85 M concentration. Lysozyme crystals were observed at 0.5 M and 0.125 M sodium malonate buffer at pH 10. Lysozyme crystals were observed at 1 M sodium chloride with PEG buffer at pH 6, 8 and 9. The number of crystals decreased as the pH of the buffer increased.

LLPS was also observed in several biochemical conditions in which polyethylene glycol is used along with the buffers. Systematically, LLPS was observed in ammonium sulfate plates. LLPS were observed at 1 M ammonium sulfate with PEG buffer at pH 5, 6, 7, 8, 9 and 10. LLPS were observed at 0.5 M ammonium sulfate with PEG buffer at pH 5, 6, 7, 8 and 9, but there was a decrease in LLPS formation as the buffer concentration decreased and pH increased. LLPS were observed at 1 M sodium chloride with PEG buffer at pH 5, 7 and 10. LLPS were observed at 0.25 M sodium chloride with PEG buffer at pH 7.

Interestingly, in some biochemical conditions we observed both LLPS and crystals. At 0.5 M concentration of ammonium sulfate with PEG as a buffer at pH 10 we observed crystals and droplets i.e, LLPS. At 1 M

concentration of sodium chloride with PEG as a buffer at pH 6 we observed crystals and LLPS. At 1 M concentration of sodium chloride with PEG as a buffer at pH 8 we observed crystals and LLPS. At 1 M concentration of sodium chloride with PEG as a buffer at pH 9 we observed crystals and LLPS.

Based on the results we observed that by using these buffers we can obtain crystals and LLPS also. In some biochemical conditions both LLPS and crystals were also observed. Now we conduct our further research at the biochemical conditions at which LLPS is observed and we avoid the biochemical conditions at which crystals are formed.

Conclusion and Future directions:

Emerging evidence suggests that LLPS is a vital and pervasive phenomenon underlying the development of membrane-less organelles in eukaryotic cells. LLPS is gaining acceptance as a powerful mechanism to explain the formation of membrane-less organelles and their functions. Recent studies have revealed evidence that LLPS plays a vital role in human health and disease. This highlights the need for an overview of the recent advances in the field to translate our current knowledge regarding LLPS into therapeutic discoveries. Condensates formed via LLPS provide specific local environments for broad cellular activities. Biomacromolecules suffer from poor cellular membrane permeability, limiting their access to intracellular targets. Strategies to overcome this challenge scientists are doing research often using LLPS for drug delivery. This research led to the platform for the drug delivery using LLPS which is effective. Hanging drop vapor diffusion technique was performed under different biochemical conditions using five different buffers with six different pH conditions and four different molarities using lysozyme. We mainly focused on the biochemical conditions at which liquid-liquid phase separation occurs and we avoid the biochemical conditions at which lysozyme crystals appear for further investigation.

We conduct our further research at the biochemical conditions at which LLPS is observed. We avoid the biochemical conditions at which crystals are formed. We continue our further research for the drug delivery using LLPS which is very useful for treating various pathologies, cancers and metabolic diseases.

Acknowledgements: We thank The Yedidi Institute of Discovery and Education, Toronto for scientific collaborations.

Conflict of interest: The authors declare no conflict of interest in this study.

Author contributions: P.L. and S.N. performed all the wet lab studies under the guidance of M.S. and R.S.Y. R.S.Y. is the principal investigator who designed the project, trained P.L., S.N. and M.S. secured required material for the project, provided the laboratory space and facilities needed. R.S.Y. wrote, edited and finalized the manuscript. All authors approve the final manuscript.

References

1. Wang, Z., Zhang, G. & Zhang, H. Protocol for analyzing protein liquid–liquid phase separation. *Biophys Rep* 5, 1–9 (2019).
2. Ming, Y., Chen, X., Xu, Y., Wu, Y., Wang, C., Zhang, T., Mao, R., & Fan, Y. (2019). Targeting liquid-liquid phase separation in pancreatic cancer. *Translational cancer research*, *8*(1), 96–103.
3. Su, X., Ditlev, J. A., Hui, E., Xing, W., Banjade, S., Okrut, J., King, D. S., Taunton, J., Rosen, M. K., & Vale, R. D. (2016). Phase separation of signaling molecules promotes T cell receptor signal transduction. *Science (New York, N.Y.)*, *352*(6285), 595–599.
4. Li, P., Banjade, S., Cheng, H. C., Kim, S., Chen, B., Guo, L., Llaguno, M., Hollingsworth, J. V., King, D. S., Banani, S. F., Russo, P. S., Jiang, Q. X., Nixon, B. T., & Rosen, M. K. (2012). Phase transitions in the assembly of multivalent signalling proteins. *Nature*, *483*(7389), 336–340.
5. Bai X, Pei P, Duan G, et al. Phase separation enhanced drug delivery system for anti-cancer therapy. Research Square; 2022.
6. Wilson, E. B. The structure of protoplasm. Science 10, 33–45 (1899).
7. Brangwynne, C. P. *et al.* Germline P granules are liquid droplets that localize by controlled dissolution/condensation. Science 324, 1729–1732 (2009).
8. Li, P. *et al*. Phase transitions in the assembly of multivalent signalling proteins. Nature 483, 336–340 (2012).
9. Wang, J. *et al.* A molecular grammar governing the driving forces for phase separation of prion-like RNA binding proteins. Cell 174, 688–699.e16 (2018).
10. Lu, S. *et al*. The SARS-CoV-2 nucleocapsid phosphoprotein forms mutually exclusive condensates with RNA and the membrane-associated M protein. Nat. Commun.12, 502 (2021).
11. Carlson, C. R. *et al*. Phosphoregulation of phase separation by the SARS-CoV-2 N protein suggests a biophysical basis for its dual functions. Mol. Cell 80,1092–1103.e4 (2020).
12. Shin, Y. *et al*. Spatiotemporal control of intracellular phase transitions using light-activated opto-droplets. Cell 168, 159–171.e14 (2017).
13. Boija, A. *et al*. Transcription factors activate genes through the phase-separation capacity of their activation domains. Cell 175, 1842–1855.e16 (2018).
14. Rougvie, A. E. & Lis, J. T. The RNA polymerase II molecule at the 5' end of the uninduced hsp70 gene of D. melanogaster is transcriptionally engaged. Cell 54,795–804 (1988).
15. Henninger, J. E. *et al*. RNA-mediated feedback control of transcriptional condensates. Cell 184, 207–225.e24 (2021).
16. Gibson, B. A. *et al*. Organization of chromatin by intrinsic and regulated phase separation. Cell 179, 470–484.e21 (2019).

17. Maison, C. & Almouzni, G. HP1 and the dynamics of heterochromatin maintenance. Nat. Rev. Mol. Cell Biol. 5, 296–304 (2004).
18. Strom, A. R. *et al*. Phase separation drives heterochromatin domain formation. Nature 547, 241–245 (2017).
19. Wang, T., Xu, C., Liu, Y., Fan, K., Li, Z., Sun, X., Ouyang, H., Zhang, X., Zhang, J., Li, Y., Mackenzie, F., Min, J., & Tu, X. (2012). Crystal structure of the human SUV39H1 chromodomain and its recognition of histone H3K9me2/3. *PloS one*, *7*(12), e52977.
20. Li, S., Balmain, A. & Counter, C. M. A model for RAS mutation patterns in cancers: finding the sweet spot. Nat. Rev. Cancer 18, 767–777 (2018).
21. Song, Y. *et al*. The emerging role of SPOP protein in tumorigenesis and cancer therapy. Mol. Cancer 19, 2 (2020).
22. Zhu, G. *et al*. Phase separation of disease-associated SHP2 mutants underlies MAPK hyperactivation. Cell 183, 490–502.e18 (2020).
23. Yu, M. *et al*. Interferon-γ induces tumor resistance to anti-PD-1 immunotherapy by promoting YAP phase separation. Mol. Cell. 81, 1216–1230.e9 (2021).
24. Romagnoli, S., Peris, A., De Gaudio, A. R. & Geppetti, P. SARS-CoV-2 and COVID19: From the Bench to the Bedside. Physiol. Rev. 100, 1455–1466 (2020).
25. Chang, C. K., Hou, M. H., Chang, C. F., Hsiao, C. D. & Huang, T. H. The SARS coronavirus nucleocapsid protein–forms and functions. Antivir. Res. 103, 39–50(2014).
26. Carlson, C. R. *et al*. Phosphoregulation of phase separation by the SARS-CoV-2 N protein suggests a biophysical basis for its dual functions. Mol. Cell 80,1092–1103.e4 (2020).
27. Iserman, C. *et al*. Genomic RNA elements drive phase separation of the SARS-CoV-2 nucleocapsid. Mol. Cell 80, 1078–1091.e6 (2020).
28. Chang, L. W. *et al*. Sequence and entropy-based control of complex coacervates. Nat Commun 8,1273 (2017).
29. Phase-separating peptides for direct cytosolic delivery and redox-activated release of macromolecular therapeutics. Yue Sun1, Sze Yi Lau, Zhi Wei Lim1, Shi Chieh Chang, Farid Ghadessy,Anthony Partridge and Ali Miserez vol 14,March 2022.
30. The structure of the hexagonal crystal form of hen egg-white lysozyme C. Brinkmann,M. S. Weissb and E. Weckerta Acta Cryst. (2006). D62, 349–355.
31. Weiss, M. S., Palm, G. J., & Hilgenfeld, R. (2000). Crystallization, structure solution and refinement of hen egg-white lysozyme at pH 8.0 in the presence of MPD. *Acta crystallographica. Section D, Biological crystallography*, *56*(Pt 8), 952–958.
32. Yamanaka, M., Inaka, K., Furubayashi, N., Matsushima, M., Takahashi, S., Tanaka, H., Sano, S., Sato, M., Kobayashi, T., & Tanaka, T. (2011). Optimization of salt concentration in PEG-based crystallization solutions. *Journal of synchrotron radiation*, *18*(1), 84–87.
33. Ries-Kautt, M. M., & Ducruix, A. F. (1989). Relative effectiveness of various ions on the solubility and crystal growth of lysozyme. *The Journal of biological chemistry*, *264*(2), 745–748.
34. Iwai, W., Yagi, D., Ishikawa, T., Ohnishi, Y., Tanaka, I., & Niimura, N. (2008). Crystallization and evaluation of hen egg-white lysozyme crystals for protein pH titration in the crystalline state. *Journal of synchrotron radiation*, *15*(Pt 3), 312–315.
35. Tanaka, Shinpei and Yamamoto, Masahiko and Ito, Kohzo and Hayakawa, Reinosuke and Ataka, Mitsuo. (1997). Relation between the phase separation and the crystallization in protein solutions. Phys. Rev. E. 56(1), R67--R69.